

# Skyrmion lattice melting in the quantum Hall system

Carsten Timm\* and S. M. Girvin

*Department of Physics, Indiana University, Bloomington, Indiana 47405*

H.A. Fertig

*Department of Physics and Astronomy, University of Kentucky, Lexington, Kentucky 40506*

(April 6, 1998)

The melting and magnetic disordering of the skyrmion lattice in the quantum Hall system at filling factor  $\nu \approx 1$  are studied. A Berezinskii-Kosterlitz-Thouless renormalization group theory is employed to describe the coupled magnetic and translational degrees of freedom. The non-trivial magnetic properties of the skyrmion system stem from the in-plane components of the non-collinear magnetization in the vicinity of skyrmions, which are described by an antiferromagnetic XY model. In a Coulomb gas formulation the ‘particles’ are the topological defects of the XY model (vortices) and of the lattice (dislocations and disclinations). The latter frustrate the antiferromagnetic order and acquire fractional vorticity in order to minimize their energy. We find a number of melting/disordering scenarios for various lattice types. While these results do not depend on a particular model, we also consider a simple classical model for the skyrmion system. It results in a rich  $T = 0$  phase diagram. We propose that the triangular and square skyrmion lattices are generically separated by a centered rectangular phase in the quantum Hall system.

PACS numbers: 73.40.Hm, 75.40.Cx, 75.70.Ak

## I. INTRODUCTION

### A. General Remarks and Motivation

For nearly two decades the study of the quantum Hall effect has been one of the most productive fields of condensed matter physics.<sup>1–5</sup> Recently, quantum Hall systems with additional degrees of freedom have received considerable attention.<sup>6–13</sup> In the simplest case this degree of freedom is the electron spin. Ideas developed for this system can be adapted for other multi-component quantum Hall systems such as coupled layers, wide quantum wells, and quantum wells in semiconductors with several degenerate conduction band minima.<sup>13</sup>

Here, we study the effect of the electron spins. We are motivated by recent nuclear magnetic resonance<sup>14</sup> and specific heat<sup>15</sup> measurements exhibiting interesting finite temperature spin physics. At the Landau level filling factor  $\nu = 1/m$ , where  $m$  is an odd integer, the ground state of the two-dimensional electron gas is a strong ferromagnet,<sup>16,13,17</sup> *i.e.*, the electronic spins are completely aligned even in the limit of vanishing Zeeman coupling. Perhaps surprisingly, the effective Zeeman field in this system is rather small because of band structure effects. In the following we consider the case  $\nu \sim 1$ . The low-energy excitations of the system at  $\nu = 1$  are spin waves gapped at the Zeeman energy. However, the quantum Hall ferromagnet also has topologically non-trivial excitations, which are (not strictly correctly) referred to as *skyrmions*<sup>18,16,10</sup> in analogy with the Skyrme model in nuclear physics.<sup>19–21</sup> They can be thermally created in pairs of vanishing topological charge, similar to vortices in two-dimensional superfluids. Skyrmions are in fact also present in conventional itinerant ferromagnets such as iron but do not seem to have any observable

consequences at low temperatures. What makes them crucial for quantum Hall ferromagnets is that the vanishing diagonal conductivity  $\sigma_{xx} = 0$  together with the finite Hall conductivity  $\sigma_{xy} = \nu e^2/h$  makes the skyrmions carry a quantized electrical charge of  $\pm \nu e$ .<sup>16,10</sup> As a result, skyrmions (or antiskyrmions) are present even in the ground state if we move slightly away from  $\nu = 1$ .<sup>22,23</sup> (For our purposes skyrmions and antiskyrmions behave identically and we refer to both as “skyrmions.”)

If one dopes electrons or holes into the two-dimensional electron gas at  $\nu = 1$ , they enter the system as skyrmions with charge  $\mp e$  but with more than one flipped spin. This effect can be seen in measurements of the magnetization as a function of filling factor.<sup>14</sup> The result is a non-collinear ground state since the magnetization in the vicinity of the skyrmion centers has components perpendicular to the magnetic field, which have a vortex-like configuration. In a collinear magnet the SO(3) spin symmetry is broken to a SO(2) symmetry with respect to rotations around the magnetic field direction. It has one Goldstone mode, which is gapped at the Zeeman energy in the presence of a magnetic field. In a non-collinear magnet the SO(2) symmetry is further broken and there are two Goldstone modes, only one of which is gapped. The other, gapless mode corresponds to rotation of the non-collinear spin configuration around the magnetic field axis. Thus non-collinearity leads to the appearance of a new low-energy SO(2)  $\sim$  U(1) degree of freedom. In the long-wavelength limit the orientation of the in-plane components of the magnetization of a skyrmion can be described by a single U(1) phase factor  $e^{i\phi}$  or by the angle  $\phi$ .

Moving further away from  $\nu = 1$ , more and more skyrmions are present and their interaction becomes important. The skyrmion interaction contains a repulsive,

long-range Coulomb part and a short-range contribution related to the U(1) degree of freedom. The latter term, which we here call the *magnetic* interaction, favors antiparallel alignment of the U(1) “spins.” Brey *et al.*<sup>23</sup> recognized that the magnetic interaction could lead to a square lattice of skyrmions instead of the usual triangular (hexagonal) lattice since the square lattice allows Néel order of the U(1) degree of freedom whereas magnetic order is frustrated on the triangular lattice. Since the magnetic interaction is of short range, the Coulomb interaction dominates for small skyrmion densities and one expects a triangular crystal. The U(1) degree of freedom is then frustrated, with neighboring angles  $\phi$  differing by  $\pm 120^\circ$ . On the other hand, if the density is sufficiently high, the energy gained from Néel ordering on the square lattice may outweigh the lost Coulomb energy. Further lattice types may also be possible, *e.g.*, a centered rectangular lattice, *i.e.*, a square lattice stretched along the (11) direction, with Néel order. In Sec. II we employ a simple classical model of the skyrmion system to illustrate which lattice types and structural transitions may be expected. We find a surprisingly rich phase diagram for the classical ground state. The classical ground state has also been investigated by Rao *et al.*<sup>24</sup> employing a non-linear sigma model and by Green *et al.*<sup>25</sup>, who also study the lattice dynamics, see Sec. II below.

If the skyrmion positions were fixed to the ideal lattice at all temperatures, the long-wavelength physics, in particular the critical properties, would be well described by an antiferromagnetic lattice XY model. We would then expect a Berezinskii-Kosterlitz-Thouless (BKT) transition,<sup>26,27</sup> which separates a low-temperature phase of bound pairs of logarithmically interacting vortices and antivortices from a high-temperature phase where large pairs are broken in the sense that their interaction is completely screened. These broken pairs, which essentially consist of free vortices and antivortices, destroy quasi-long-range order. In the skyrmion lattice, however, the positions are not fixed and the lattice itself can melt.

The critical properties of a two-dimensional lattice without any internal degree of freedom have been successfully described by Nelson and Halperin<sup>28</sup> and by Young<sup>29</sup> applying BKT theory to dislocations and disclinations of the lattice. Melting of the triangular and square lattices proceeds in two steps, both well described by BKT theory,<sup>28</sup> unless one or both of these transitions is preempted by a first-order melting transition. At the lower transition bound pairs of dislocations with opposite Burger’s vector decouple, leading to a liquid crystal phase with short-range translational order but persisting quasi-long-range orientational order of nearest-neighbor bonds. Note that dislocations are, like vortices, topological defects with logarithmic bare interaction. For the triangular lattice, the liquid crystal phase is called *hexatic* because it shows quasi-long-range order with respect to a sixfold rotational symmetry, whereas for the square lattice it is called *tetratic* (fourfold symmetry).<sup>28</sup> However, the square lattice is unstable in a system with Coulomb

repulsion as the only interaction. At the higher transition temperature, pairs of disclinations, *i.e.*, defects in the bond orientation field, unbind, leading to an isotropic fluid. The *bare* disclination interaction is confining but the presence of free dislocations above the lower melting temperature leads to a logarithmic interaction.<sup>28</sup>

For the skyrmion lattice, the U(1) degree of freedom may not only stabilize the square lattice structure,<sup>23</sup> we also expect the short-range magnetic interaction to be strongly affected by lattice deformations, leading to the coupling of magnetic and lattice degrees of freedom. There are two aspects to this coupling: First, the low-energy collective modes (XY spin waves and lattice vibrations) may be coupled. From general arguments<sup>30,17,31</sup> the dispersion of the lattice vibration mode, usually called *magnetophonon* mode, close to the Brillouin zone center is expected to have the form  $\omega \propto k^{3/2}$ . Côté *et al.*<sup>17</sup> have performed time-dependent Hartree-Fock calculations for the collective mode spectrum of square skyrmion crystals. The authors indeed find two distinct low-energy branches. One is linear in  $\mathbf{k}$  and is interpreted as the gapless XY spin wave mode, whereas the other has the  $k^{3/2}$  magnetophonon dispersion. There is no sign of mixing of these two modes at small  $k$ . In Sec. II C we briefly show that the classical skyrmion model reproduces these features.

Second, despite the fact that the collective modes are largely decoupled, the topological excitations (vortices, dislocations, and disclinations) may be coupled, leading to an interplay of the magnetic BKT transition and the BKT melting transitions. That something non-trivial happens is easily seen from Fig. 1: A dislocation in a square lattice leads to a phase mismatch of  $\pm\pi$  in the U(1) degree of freedom since the nearest-neighbor coupling is antiferromagnetic. Naively one could expect that this mismatch along the dashed line in Fig. 1 leads to a linear, confining term in the interaction of a dislocation pair. However, the magnetization can relax so as to minimize the mismatch energy, as shown in Fig. 1(b). In this relaxed configuration, the dislocation has acquired *half* a U(1) vortex and the dislocation interaction is again logarithmic. The main objective of this paper is to illustrate this point further and to explore its consequences for melting and magnetic disordering of various skyrmion lattice types.

The vorticity acquired by dislocations can be derived using a gauge theory of elasticity following ideas of Cardy *et al.*<sup>32</sup>, who have studied a soft square lattice of antiferromagnetically coupled Ising spins. Dislocations frustrate the antiferromagnetic order in this system as well. In Sec. I B we sketch the gauge theory for the case of a square skyrmion lattice.

Experimentally, the situation is less clear. The presence of skyrmions for  $\nu \approx 1$  but  $\nu \neq 1$  is firmly established by magnetization measurements by Barrett *et al.*<sup>14</sup>, using optically pumped nuclear magnetic resonance (NMR) techniques. Less certain, the very large nuclear relaxation rate  $T_1^{-1}$  seen in this regime<sup>14</sup> is interpreted in

terms of the gapless  $XY$  magnon mode.<sup>17</sup> This mode couples strongly to the nuclear spins because of its large  $S^{x,y}$  components and its gaplessness. This coupling opens a channel for rapid spin-lattice relaxation of nuclear spins. In these experiments<sup>14</sup> the skyrmions are probably usually in a liquid state. Nevertheless the gapless  $XY$  mode is presumably still present as an overdamped mode.

Bayot *et al.*<sup>15</sup> find a strongly enhanced specific heat  $C$  for  $\nu \approx 1$ , which suggests strong coupling between electronic and nuclear spins so that the large specific heat of the nuclear spins is in fact measured. Again, a plausible coupling mechanism is provided by the gapless  $XY$  magnons. The filling factor dependence of  $C$  is consistent with this picture.<sup>15</sup> The temperature dependence of  $C$  shows a sharp peak at very low  $T$ . This peak may indicate a skyrmion lattice melting transition. Our so far quite speculative interpretation is the following: Neglecting the skyrmions for a moment, the Zeeman energy of nuclear spins within the quantum well containing the two-dimensional electron gas is (Knight) shifted because of their coupling to the polarized electron gas. Outside of the quantum well there is no such Knight shift and the mismatch in the Zeeman energy prevents the spins within and outside of the well from coming into thermal equilibrium. If skyrmions are present in a liquid state they move around, leading to motional narrowing and an averaged, but still finite, Knight shift within the well. In a lattice state, however, there are regions around the skyrmions where the electronic magnetization is perpendicular to the external field and the Knight shift vanishes. The nuclear spins outside of the well can come into equilibrium with the nuclei in these regions. Hence, specific heat measurements suddenly see the nuclei outside of the quantum well when a skyrmion lattice forms. Below the transition the apparent specific heat drops off again, which may indicate that the coupling is strong only in the vicinity of the transition where critical slowing down causes the electronic motion time scale to pass through the NMR time scale. To our knowledge, these experiments<sup>15</sup> are the only ones showing signs of a finite-temperature phase transition in a single-layer quantum Hall system. Recent experiments using resonant inelastic light scattering off *double-layer* systems<sup>11</sup> also show signs of a finite-temperature transition.<sup>11,12</sup>

The objective of this paper is to illustrate several of the points raised above, in particular we wish to explore the consequences of the vorticity acquired by lattice defects for the melting and magnetic disordering transitions of skyrmion lattices. In Sec. III we study these transitions for several possible lattice types. We introduce a generalized BKT renormalization group theory for a Coulomb gas with more than one species of particle carrying more than one kind of charge. The specific lattice types we study are motivated by the possible ground states of the simple classical skyrmion model of Sec. II. It should be kept in mind, however, that the BKT theory does not depend on any particular model.

## B. Gauge Theory of Elasticity for the Skyrmion Lattice

Following Cardy *et al.*<sup>32</sup> we here formulate a gauge theory for the magnetic and elastic energy of a square skyrmion lattice, *i.e.*, a soft square lattice with an  $XY$  degree of freedom. Other skyrmion lattice types can be treated similarly. Let  $S(\mathbf{R}) \equiv e^{i\phi(\mathbf{R})}$  be the  $XY$  spin field, where  $\mathbf{R}$  is a lattice vector. We define a magnetic order parameter

$$\Phi(\mathbf{R}) \equiv S(\mathbf{R}) e^{i\pi(r_x+r_y)/a}, \quad (1)$$

where  $\mathbf{r}(\mathbf{R})$  is the actual position of the skyrmion belonging to the ideal lattice vector  $\mathbf{R}$  and  $a$  is the lattice constant. This picture breaks down in the presence of free disclinations, *i.e.*, above the upper melting transition, because then the  $x$  and  $y$  components of the position vector  $\mathbf{r}$  are no longer well-defined. The additional phase factor turns the spins on one sublattice through  $\pi$ , thereby mapping the antiferromagnet onto a ferromagnet. In the presence of dislocations this is not possible: The phase factor is no longer unique and  $\Phi(\mathbf{R})$  cannot be both continuous and single-valued. Using a continuum notation, the exchange energy is

$$H_{\text{ex}} = \int d^2R \rho (\nabla\Phi)^* (\nabla\Phi). \quad (2)$$

Next, we define two translational order parameters

$$\Psi_x(\mathbf{R}) \equiv e^{i2\pi r_x/a}, \quad (3)$$

$$\Psi_y(\mathbf{R}) \equiv e^{i2\pi r_y/a}. \quad (4)$$

Although  $\mathbf{r}(\mathbf{R})$  is not continuous and single-valued in the presence of dislocations, the fields  $\Psi_{x,y}$  are. Continuum elastic theory yields the elastic energy of a square lattice,<sup>33</sup>

$$H_{\text{el}} = \int d^2R \left( \mu u_{ij} u_{ij} + \frac{\lambda}{2} u_{ii} u_{jj} + \nu u_{xx} u_{yy} \right) \quad (5)$$

where summation over repeated indices is implied and

$$u_{ij} \equiv \frac{1}{2} \left( \frac{\partial r_i}{\partial R_j} + \frac{\partial r_j}{\partial R_i} \right). \quad (6)$$

The last term in the elastic energy would be absent for a triangular crystal or an isotropic medium.<sup>33</sup> Expressing the  $u_{ij}$  in terms of derivatives of the fields  $\Psi_{x,y}$  and integrating by parts, the elastic energy becomes

$$\begin{aligned} H_{\text{el}} = \int d^2R \frac{a^2}{8\pi^2} & \left( \mu (\nabla\Psi_i)^* (\nabla\Psi_i) \right. \\ & + (\mu + \lambda) \left[ (\partial_x\Psi_x)^* (\partial_x\Psi_x) + (\partial_y\Psi_y)^* (\partial_y\Psi_y) \right] \\ & + (\mu + \lambda + \nu) \left[ \Psi_x (\partial_x\Psi_x)^* \Psi_y^* (\partial_y\Psi_y) \right. \\ & \left. \left. + \Psi_y (\partial_y\Psi_y)^* \Psi_x^* (\partial_x\Psi_x) \right] \right). \quad (7) \end{aligned}$$

The long-range Coulomb repulsion in the skyrmion lattice drives the Lamé coefficient  $\lambda$  to infinity—the lattice is incompressible.<sup>34,35</sup> Thus only the first term on the right-hand side of Eq. (7) is relevant (the other terms may introduce constraints on  $\Psi_{x,y}$ , which we ignore in the following since they do not affect our argument).

A translation in the  $x$  ( $y$ ) direction leads to phase factors in  $\Psi_x$  ( $\Psi_y$ ) and in  $\Phi$ . A spin rotation leads to a phase factor in  $\Phi$  alone. We can express the symmetries under translation and spin rotation as *gauge symmetries*: We introduce three two-component gauge fields  $\mathbf{A}_0$ ,  $\mathbf{A}_x$ , and  $\mathbf{A}_y$  and write the energy  $H \equiv H_{\text{ex}} + H_{\text{el}}$  as

$$H = \int d^2R \left[ \rho \left| \left( \nabla - i\mathbf{A}_0 - \frac{i}{2}\mathbf{A}_x - \frac{i}{2}\mathbf{A}_y \right) \Phi \right|^2 + \frac{a^2\mu}{8\pi^2} |(\nabla - i\mathbf{A}_x)\Psi_x|^2 + \frac{a^2\mu}{8\pi^2} |(\nabla - i\mathbf{A}_y)\Psi_y|^2 \right]. \quad (8)$$

This Hamiltonian is invariant under gauge transformations with respect to any of the three gauge fields:

$$\mathbf{A}_0 \rightarrow \mathbf{A}_0 + \nabla\theta_0, \quad \Phi \rightarrow e^{i\theta_0} \Phi, \quad (9)$$

$$\mathbf{A}_x \rightarrow \mathbf{A}_x + \nabla\theta_x, \quad \Phi \rightarrow e^{i\theta_x/2} \Phi, \quad \Psi_x \rightarrow e^{i\theta_x} \Psi_x, \quad (10)$$

$$\mathbf{A}_y \rightarrow \mathbf{A}_y + \nabla\theta_y, \quad \Phi \rightarrow e^{i\theta_y/2} \Phi, \quad \Psi_y \rightarrow e^{i\theta_y} \Psi_y. \quad (11)$$

These three transformations correspond to spin rotation, translation in the  $x$  direction, and translation in the  $y$  direction, respectively. The *matter fields*  $\Phi$ ,  $\Psi_x$ , and  $\Psi_y$  in the Hamiltonian, Eq. (8), are only coupled through the gauge fields.

We now discuss the topological defects in this theory. Magnetic vortices, *i.e.*, vortices in  $\Phi$ , are threaded by one flux quantum with regard to  $\mathbf{A}_0$ . Dislocations correspond to topological defects in  $\Psi_x$  or  $\Psi_y$ , depending on the Burger's vector orientation. The elementary defect in, say,  $\Psi_x$  is a unit vortex. It is threaded by one flux quantum in  $\mathbf{A}_x$ . This seems to make the field  $\Phi$  multi-valued since its phase changes by  $\pi$  if one moves around the vortex. However, if the  $XY$  spin part  $S$  in  $\Phi$  itself contains *half* a vortex (or antivortex) the order parameter  $\Phi$  is again single-valued and continuous. This corresponds to  $\pm 1/2$  flux quanta in  $\mathbf{A}_0$ . Thus we reobtain the result already discussed in Sec. IA: Dislocations each acquire  $\pm 1/2$  magnetic vortex.

## II. CLASSICAL MODEL FOR THE SKYRMION LATTICE

In the present section we formulate a simple classical model for the interacting skyrmion system. We use this model to obtain (a) the classical ground state of the skyrmion lattice for a wide range of values of the skyrmion density and the magnetic interaction strength, and (b) the spectrum of low-lying collective excitations. This model should represent the physics of the real

skyrmion lattice at least qualitatively, and even quantitatively at low density. This section is meant to illustrate some of the properties to be expected for the skyrmion lattice without introducing irrelevant technical complications. Furthermore, we wish to motivate the choice of lattice types studied on a more general level in Sec. III.

### A. Model

The main idea is to take the correct limit of the two-skyrmion interaction at large distances and treat the skyrmion system as a classical gas of point particles having this interaction at all separations. We thus keep only the respective leading-order terms for large separations of both the interaction contribution independent of the  $XY$  degree of freedom and of the contribution depending on this degree of freedom, and we neglect three-, four-, etc. body interactions. This model should be valid at low skyrmion densities.

We start from the classical non-linear sigma model for the magnetization,<sup>36,37</sup> which has been successfully applied to quantum Hall ferromagnets.<sup>16,10</sup> Abolfath *et al.*<sup>38</sup> have recently discussed the applicability of this classical field theory and compared its predictions with microscopic results. The magnetization is represented by a normalized three-component vector field  $\mathbf{m}(\mathbf{r})$ . The relevant terms in the Lagrangian read

$$L = \frac{\hbar}{4\pi\ell^2} \int d^2r \mathbf{A}[\mathbf{m}] \cdot \partial_t \mathbf{m} - \frac{\rho_s}{2} \int d^2r (\partial_i m_\mu)(\partial_i m_\mu) + \frac{\rho g^* \mu_B B}{2} \int d^2r m_3(\mathbf{r}) - \frac{e^2}{2\epsilon} \int d^2r d^2r' \delta\rho(\mathbf{r}) \frac{1}{|\mathbf{r} - \mathbf{r}'|} \delta\rho(\mathbf{r}'), \quad (12)$$

where  $\mathbf{A}[\mathbf{m}]$  is the vector potential of a magnetic monopole at the origin in spin ( $\mathbf{m}$ ) space,<sup>13</sup>  $\partial_t$  is a time derivative, and

$$\delta\rho \equiv -\frac{1}{8\pi} \epsilon_{ij} \mathbf{m} \cdot (\partial_i \mathbf{m} \times \partial_j \mathbf{m}) \quad (13)$$

is the topological (Pontryagin) density. Greek indices always run over three values and latin ones over two. The first term is the usual Berry phase, and the other three stem from exchange, Zeeman, and Coulomb interaction, respectively. The Coulomb term reflects the fact that skyrmions carry electrical charge.

In the absence of Zeeman and Coulomb interactions, the ground-state solution for a single skyrmion is known analytically.<sup>20</sup> It is scale invariant and for large distances  $r = |\mathbf{r}|$  from the skyrmion center the in-plane components of  $\mathbf{m}$  fall off as  $m_j \propto r_j/r^2$ . Rotation around the  $z$  axis gives a *different* ground-state solution, reflecting the completely broken  $SO(3)$  symmetry.

Switching on the Zeeman interaction, scale invariance is broken since the Zeeman term prefers a small skyrmion.

Far away from the skyrmion center we can expand the exchange and Zeeman terms in the Lagrangian, Eq. (12), up to second order in the small in-plane components  $m_j$  of the magnetization,<sup>31</sup>

$$E \cong \int d^2r \left[ \frac{\rho_s}{2} (\partial_i m_j)(\partial_i m_j) + \frac{\rho g^* \mu_B B}{2} m_j m_j \right]. \quad (14)$$

The resulting Euler-Lagrange equation

$$-\partial_i \partial_i m_j + \frac{\rho g^* \mu_B B}{2} m_j = 0 \quad (15)$$

has a vortex solution with<sup>31</sup>

$$m_j \propto \frac{r_j}{r^{3/2}} e^{-\kappa r} \quad (16)$$

for  $j = 1, 2$ . This expression is valid for  $r \gg 1/\kappa$ , where  $\kappa^2 = \rho g^* \mu_B B / 2\rho_s$ . Again the in-plane components can be rotated through any angle  $\phi$ . By inserting  $\mathbf{m}$  into Eq. (12) it is seen that the energy-density contributions of both the exchange and the Zeeman term fall off as  $r^{-1}e^{-2\kappa r}$ . Taking the Coulomb interaction into account, its leading-order contribution to the energy density also behaves like  $r^{-1}e^{-2\kappa r}$ . Thus all three energy contributions are equally relevant at large  $r$  and Coulomb interaction does not destroy the functional form of Eq. (16) but does change the value of  $\kappa$ .

In calculating the interaction energy we assume that the two-skyrmion state with one skyrmion at the origin and the other at  $\mathbf{s}$  is well described by

$$m_j(\mathbf{r}) = m_j^{\text{single}}(\mathbf{r}) + R_{jk}(\phi) m_k^{\text{single}}(\mathbf{r} - \mathbf{s}) \quad (17)$$

for  $j = 1, 2$ . The component  $m_3$  is determined by  $|\mathbf{m}| = 1$ . This ansatz only gives errors of higher order in  $e^{-\kappa s}$  for large separations. Here,

$$R_{jk}(\phi) = \begin{pmatrix} \cos \phi & \sin \phi \\ -\sin \phi & \cos \phi \end{pmatrix} \quad (18)$$

rotates the in-plane  $\mathbf{m}$  components of one of the skyrmions through an angle  $\phi$ . We find the interaction potential by inserting  $\mathbf{m}$  into the potential energy part of Eq. (12) and subtracting the energies of two isolated skyrmions. We are interested in the limiting form for large separations  $s$ .

The exchange contribution to the interaction is the only one depending on the angle  $\phi$ . Using a multipole expansion and integrating over  $\mathbf{r}$  we find, to leading order, the exchange contribution  $E_{\text{exch}} \propto \cos \phi e^{-\kappa s} / \sqrt{s}$ , where the coefficient of proportionality is positive. The contribution from the Zeeman term does not depend on  $\phi$  and is exponentially small for large separations. We neglect it compared to the Coulomb interaction, below, since we only keep the leading  $\phi$  dependent and the leading  $\phi$  independent term. For  $\nu = 1$  the leading contribution from the Coulomb interaction is  $e^2/\epsilon s$ , where  $\epsilon$  is the dielectric constant of the material. There are higher multipole terms, which fall off at least as  $1/s^3$  and are neglected compared to the  $1/s$  term.

## B. Ground states

As long as the skyrmion density is small, we expect the interaction to be dominated by the two-particle large-separation terms found above. Our approximation for the energy per skyrmion of a skyrmion lattice is

$$E = E_C + E_{XY} \quad (19)$$

with

$$E_C = \frac{e^2}{2\epsilon} \sum_{\mathbf{R} \neq 0} \frac{1}{R} - E_0, \quad (20)$$

$$E_{XY} = \frac{g_{XY}}{2} \sum_{\mathbf{R} \neq 0} \cos(\phi_{\mathbf{R}} - \phi_0) \frac{e^{-R/\xi_{XY}}}{\sqrt{R}}, \quad (21)$$

where  $\mathbf{R}$  runs over all skyrmion positions in the lattice except  $\mathbf{R} = 0$ ,  $E_0$  is an infinite constant from the Coulomb interaction with the neutralizing background,  $g_{XY} > 0$  denotes the strength of the magnetic interaction,  $\phi_{\mathbf{R}}$  is the angle of rotation of the skyrmion at  $\mathbf{R}$ , and  $\xi_{XY} \equiv 1/\kappa$  is the range of the magnetic interaction.

The long-range Coulomb interaction is not easy to sum over. The main idea of how to make this summation well-behaved is due to Ewald<sup>39</sup> and has been successfully applied to two-dimensional crystals:<sup>40,35,41</sup> The lattice sum is split into a rapidly converging part and a long-range part, which is mapped onto a rapidly converging sum over the reciprocal lattice. Here, we quote a more general result,<sup>40,41</sup> which will be useful later: If the  $\mathbf{R}$  are summed over a two-dimensional Bravais lattice then

$$\begin{aligned} e^{i\mathbf{k}\cdot\mathbf{s}} \sum_{\mathbf{R}} \frac{e^{-i\mathbf{k}\cdot(\mathbf{R}+\mathbf{s})}}{|\mathbf{R}+\mathbf{s}|} - \frac{1}{s} &= \sqrt{n} \sum_{\mathbf{G}} e^{i(\mathbf{G}+\mathbf{k})\cdot\mathbf{s}} \Phi\left(\frac{|\mathbf{G}+\mathbf{k}|^2}{4\pi n}\right) \\ &+ \sqrt{n} \sum_{\mathbf{R} \neq 0} e^{-i\mathbf{k}\cdot\mathbf{R}} \Phi(\pi n |\mathbf{R}+\mathbf{s}|^2) \\ &+ \sqrt{n} \Phi(\pi n s^2) - \frac{1}{s}, \end{aligned} \quad (22)$$

where  $\mathbf{G}$  are the reciprocal lattice vectors,  $n$  is the number density, and  $\Phi(x) \equiv \sqrt{\pi/x} \operatorname{erfc}(\sqrt{x})$  with the complementary error function  $\operatorname{erfc}$ .<sup>42</sup> Equation (22) only works for a Bravais lattice, lattices with a basis need special consideration. The magnetic structure is irrelevant here, since the Coulomb interaction does not depend on  $\phi_{\mathbf{R}}$ .

The simple sum over Coulomb interactions is obtained in the limit  $\mathbf{s} \rightarrow 0$ ,  $\mathbf{k} \rightarrow 0$ , where the two sums on the right hand side can be cast into one,

$$E_C = \frac{e^2}{\epsilon} \sum_{\mathbf{R} \neq 0} \frac{\operatorname{erfc}(\sqrt{\pi n} R)}{R} - \frac{2e^2 \sqrt{n}}{\epsilon}. \quad (23)$$

Now all lattice sums are rapidly converging and we can calculate the energy accurately. We write the energy per skyrmion in a dimensionless form,

$$\tilde{E} \equiv \frac{E}{e^2 \epsilon^{-1} \sqrt{n}} = \sum_{\mathbf{r} \neq 0} \frac{\text{erfc}(\sqrt{\pi} r)}{r} - 2 + \frac{1}{2\alpha} \sum_{\mathbf{r} \neq 0} \cos(\phi_{\mathbf{r}} - \phi_0) \frac{e^{-r/\beta}}{\sqrt{r}} \quad (24)$$

with

$$\mathbf{r} \equiv \sqrt{n} \mathbf{R}, \quad (25)$$

$$\alpha \equiv e^2 n^{1/4} / \epsilon g_{XY}, \quad (26)$$

$$\beta \equiv \sqrt{n} \xi_{XY}, \quad (27)$$

which are all dimensionless. Note that  $\beta^2$  is the density in units derived from the range of the magnetic interaction and  $\beta/\alpha^2 = \xi_{XY} g_{XY}^2 \epsilon^2 / e^4$  is a measure of the relative strength of the magnetic interaction and does not depend on density. We expect this model to be quantitatively correct for small densities,  $\beta^2 \ll 1$ .

The classical ground state for given  $\alpha, \beta$  is determined by minimizing the energy (24). Thus we have to compare  $\tilde{E}$  for all reasonable two-dimensional lattice structures, taking the magnetic order into account. Besides the triangular lattice with frustrated antiferromagnetic order and the square lattice with Néel order<sup>23</sup> we have also obtained ground state energies for the simple rectangular, the centered rectangular, and the oblique lattice, thereby covering all two-dimensional Bravais lattices,<sup>40</sup> all with Néel order, and the honeycomb lattice, which is also bipartite but is not a Bravais lattice. We cannot strictly exclude the possibility of more complicated ground states but have not found any other likely candidate. In the cases of the rectangular and oblique lattices, the lattice is characterized by one and two, respectively, continuous parameters in addition to its space group (Bravais lattice type). For example, the simple rectangular lattice has the anisotropy  $\eta$ , defined as the ratio of the lattice constants in the (10) and (01) directions, as an additional parameter. To find the ground state, these parameters have to be optimized.

Equation (23) is not applicable to the honeycomb lattice since it is not a Bravais lattice. However, its Coulomb energy  $E_C^H$  can be expressed in terms of the triangular-lattice Coulomb energy  $E_C^T$ .<sup>43</sup> Taking the different densities into account, we find the dimensionless energy  $\tilde{E}_C^H = (1 + \sqrt{3}) / (2\sqrt{2}) \tilde{E}_C^T$ . The Coulomb energies of the parameter-free lattices are  $\tilde{E}_C^S = -1.95013$  for the square lattice,  $\tilde{E}_C^T = -1.96052$  for the triangular lattice, and  $\tilde{E}_C^H = -1.89371$  for the honeycomb lattice. The first two were also found in Ref. 40.

We map out the ground-state phase diagram in Fig. 2 by following the various transition lines, *i.e.*, lines of equal energy of two lattice types.<sup>43</sup> We then discard lines that do not separate two regions with different *ground* states. The thin lines denote continuous transitions, whereas the heavy lines show first-order transitions.<sup>43</sup> Recall that our approximation becomes doubtful for  $\beta^2 \sim 1$ , *i.e.*, towards the right edge of the diagram.

The phase diagram, Fig. 2, is quite rich. For example, there is a region where the ground state is a honeycomb lattice. In its region of stability, it is even less frustrated than the square lattice for our model interaction. In the upper left corner we find a very anisotropic ground state consisting of widely separated chains of skyrmions. Another interesting feature is the critical point on the square-simple rectangular line. Probably more relevant for real systems is the appearance of a centered rectangular phase (a square lattice stretched along the diagonal) everywhere between the triangular and square lattices. It should be possible to experimentally see this two-step transition upon varying  $\nu$ . Real skyrmion systems probably live in the lower part of the phase diagram since the magnetic interaction cannot be made arbitrarily large in experiment. The parameter  $\beta/\alpha^2$  can be increased by reducing the Zeeman interaction and thereby increasing the skyrmion size  $\xi_{XY}$ . Experimentally, this can be done by applying hydrodynamic pressure. It is easier to increase the Zeeman interaction, reducing  $\beta/\alpha^2$ , by applying an in-plane magnetic field component. We roughly estimate that  $\beta/\alpha^2$  is smaller than unity in real systems. The transition lines show an upturn to larger magnetic interactions at the right edge of the phase diagram, Fig. 2. Although this may be an artifact of our approximation  $\beta^2 \ll 1$ , it is interesting to note that a similar reentrance of a triangular phase is found in Ref. 24.

The phase diagram is rather robust against changes in the exact form of the magnetic interaction. For example, the phase diagram for a simple exponential magnetic interaction is qualitatively identical to Fig. 2. This robustness indicates that the errors made by neglecting higher-order terms in the magnetic interaction are typically small.

Rao *et al.*<sup>24</sup> use a variational classical non-linear sigma model approach to find the classical ground states of the skyrmion lattice. They only consider the square and triangular lattices and consequently do not find the other phases, in particular the centered rectangular lattice. Their method has the advantage that the skyrmion size is optimized for given density and lattice type. The single skyrmion magnetization used in Ref. 24 does not approach the correct limit at large distances but according to the above argument this should not change the results qualitatively. However, at low density a *ferromagnetically* ordered triangular lattice is found<sup>24</sup> which appears to be inconsistent with the large separation limit of the exchange interaction, Eq. (21).

### C. Dynamics

We now briefly turn to the low-energy collective excitations of the skyrmion lattice. As noted above, the U(1) degree of freedom leads to the appearance of a gapless XY spin wave mode, whereas displacements of the skyrmions lead to a magnetophonon mode. The usual

ferromagnetic spin wave mode is gapped at the Zeeman energy. This mode is expected to mix with the  $XY$  mode, except at  $\mathbf{k} = 0$ . This effect cannot be reproduced by the present model where the  $S^z$  spin components are completely integrated out. Thus the magnon dispersion is only reliable for the long-wavelength acoustical modes.

We denote the displacements of skyrmions from their ground state positions by  $\mathbf{u} = (u_1, u_2)$  and the deviation of the angle  $\phi$  from its ground state by  $u_0$ . Then we expand the potential energy Eq. (19) up to second order in  $u_\mu$ . To describe dynamics we also have to know the leading time-derivative terms in the Lagrangian. The term for displacements can be derived from the original Lagrangian, Eq. (12).<sup>44,31</sup> In the limit of vanishing Landau level mixing the skyrmion mass vanishes so that the Berry phase term is the only relevant one. One does not normally find a second-order time derivative term in spin dynamics, but Hartree-Fock calculations<sup>17</sup> clearly show that  $u_0$  obtains a mass, or rather a moment of inertia  $I$ . This can be understood as arising from having integrated out all the short-wavelength spin fluctuations in order to obtain an effective action for the collective coordinate  $u_0$ . There is also a Berry phase term associated with  $u_0$  but it is a total time derivative and thus irrelevant at the classical level. The kinetic terms in the Lagrangian are thus

$$T = \frac{I}{2} \sum_{\mathbf{R}, n} \dot{u}_0^n(\mathbf{R}) \dot{u}_0^n(\mathbf{R}) + \frac{\eta}{2} \sum_{\mathbf{R}, n} \epsilon_{ij} u_i^n(\mathbf{R}) \dot{u}_j^n(\mathbf{R}). \quad (28)$$

Here,  $\mathbf{R}$  is a Bravais lattice vector of the *magnetic* lattice, the superscript  $n = 0, 1, \dots$  selects one skyrmion of the lattice basis,  $I$  is the moment of inertia of  $u_0^n(\mathbf{R})$ , and the coefficient  $\eta$  is<sup>44,31</sup>  $\eta = e^* B$ , where  $e^* = \pm e$  is the skyrmion charge. Deriving the Euler-Lagrange equations and making a plane-wave ansatz,

$$u_\mu^n(\mathbf{R}) = A_\mu^n e^{-i(\mathbf{k} \cdot \mathbf{R} - \omega t)}, \quad (29)$$

we find the equations of motion<sup>43</sup>

$$0 = \begin{cases} I\omega^2 A_0^n & \text{for } \mu = 0 \\ -i\eta\omega\epsilon_{\mu j} A_j^n & \text{for } \mu \neq 0 \end{cases} - \sum_{n'} \left[ K_{\mu\nu}^{nn'}(0) A_\nu^n - K_{\mu\nu}^{nn'}(\mathbf{k}) A_\nu^{n'} \right] \quad (30)$$

with the dynamical matrix

$$K_{\mu\nu}^{nn'}(\mathbf{k}) \equiv \sum_{\mathbf{R}} e^{-i\mathbf{k} \cdot \mathbf{R}} \frac{\partial^2}{\partial s_\mu \partial s_\nu} \times E(\mathbf{R} + \mathbf{c}^n - \mathbf{c}^{n'} + \mathbf{s}, \phi^n - \phi^{n'} + s_0) \Big|_{\mathbf{s}=0, s_0=0}. \quad (31)$$

Here,  $E$  is the potential energy per skyrmion, Eq. (19),  $\mathbf{c}^n$  denotes the position of skyrmion  $n$  within the unit cell, and  $\phi^n$  is its  $XY$  angle.

We can now address the question of mixing of magnetophonon and  $XY$  magnon modes. Matrix elements mixing displacements and rotations of the  $XY$  angle ( $\mu = 0$

and  $\nu \neq 0$  or *vice versa*) stem from the magnetic interaction alone and contain a first-order derivative of  $\cos(\phi^n - \phi^0)$ , *i.e.*,  $\sin(\phi^n - \phi^0)$ , as a factor. Thus for any lattice with  $\phi^n \in \{0, \pi\}$  (square, rectangular, oblique, honeycomb) these matrix elements vanish. Of the lattices considered above, only the triangular shows any mixing of  $XY$  magnons and magnetophonons in our model.

Here we only show results for the square lattice. The contribution from the magnetic interaction can be summed directly, whereas for the Coulomb interaction we need the second derivatives of Eq. (22). The magnetophonon and  $XY$  magnon dispersions for  $\beta^2 = 0.1$  and  $\beta/\alpha^2 = 1$  are shown along directions of high symmetry in the magnetic Brillouin zone in Fig. 3. There are only two instead of four magnetophonon modes in the magnetic (folded-back) zone since  $u_1^n$  and  $u_2^n$  are canonically conjugate and thus do not lead to independent modes. The dispersion of the lower magnetophonon mode for small  $\mathbf{k}$  is indeed of the form  $\omega \propto k^{3/2}$ , whereas the magnon mode is linear. Note that the optical magnetophonon branch shows a minimum at the zone center, a feature previously seen in Hartree-Fock calculations.<sup>17,45</sup> We see that our simple model reproduces the main qualitative features of the collective mode spectrum and conclude that it captures the essential physics.

The dispersion relations can be used to reintroduce at least part of the quantum effects into our model by taking the zero-point energy  $\hbar\omega/2$  for all modes into account.<sup>40</sup> This additional energy may favor certain lattice types and thus shift the transition lines. It may also lead to quantum melting. Furthermore, we could extract low-temperature thermodynamic properties, such as the free energy, and with its help study structural phase transitions at finite temperatures. The harmonic approximation is, in principle, inconsistent with the description of melting, be it quantum or thermal, which is intrinsically non-linear. Nevertheless, estimates of melting temperatures could be found by calculating the amplitude of vibrations in this approximation and using a Lindemann-type criterion.<sup>41</sup> In particular, we expect quantum melting due to soft modes in the vicinity of the continuous transition lines, *e.g.*, the one between square and centered rectangular lattices.

The magnon and magnetophonon dispersions have also been studied by Green *et al.*<sup>25</sup> This work is not easily comparable to real systems since the authors assume that the skyrmion shape is little affected by Zeeman and Coulomb interactions, which yields an incorrect expression for the interaction at large distances. Furthermore, they introduce a mass term into the displacement equation of motion and their magnetophonon frequencies are inversely proportional to the mass, which seems doubtful since the mass vanishes for vanishing Landau level mixing so that the physics is dominated by the Berry phase term. Two lattice types are considered in Ref. 25: what we call the square lattice and the centered rectangular lattice, the latter with the angle between primitive lattice vectors fixed to  $\pi/3$ . The latter is structurally

identical to the triangular lattice but has only two magnetic sublattices. The authors dispute the existence of a frustrated triangular phase<sup>23</sup> but since they do not consider a triangular lattice with a three-skyrmion basis it is clear that they cannot find it.

If we go to higher temperatures, the harmonic approximation breaks down. In particular, topological excitations become important. They are believed to lead to the ultimate melting of the skyrmion crystal. In the following section we describe possible scenarios of melting.

### III. BEREZINSKII-KOSTERLITZ-THOULESS THEORY FOR SKYRMION LATTICE MELTING

In the present section, the central one of this paper, we discuss the melting transitions and intermediate phases of the lattice types discussed above. We use the framework of a suitably generalized BKT renormalization group theory<sup>26,27,46</sup> since this theory is known to work well for the simpler problems of (i) an  $XY$  model on a rigid lattice and (ii) a soft lattice without additional degrees of freedom.<sup>28,29</sup> More specifically, we employ a Coulomb gas language. BKT theory is a *static* theory so that the unconventional kinetic terms in the skyrmion Lagrangian, see, *e.g.*, Eq. (28), do not affect the results. We stress that this approach does not make reference to any special model for the interacting skyrmion system. There is one important caveat: The theory of Refs. 28 and 29 describes the system well *if* it shows BKT melting but does not say whether it actually does. The upper or both BKT melting transitions may be preempted by a first-order transition.

#### A. Multiple-charge Coulomb gas

We first introduce a general model, which contains all relevant skyrmion lattices as special cases. This model is a two-dimensional continuum Coulomb gas with more than one species of particles carrying more than one charge. The dislocations and vortices are treated as classical point particles with logarithmic interactions. From continuum elasticity theory one finds that for the triangular lattice the interaction between two dislocations with Burger's vectors  $\mathbf{b}_1$  and  $\mathbf{b}_2$  and separation vector  $\mathbf{r}$  is proportional to<sup>47,28,29,35</sup>

$$-\mathbf{b}_1 \cdot \mathbf{b}_2 \ln \frac{|\mathbf{r}|}{\tau} + \frac{(\mathbf{b}_1 \cdot \mathbf{r})(\mathbf{b}_2 \cdot \mathbf{r})}{\mathbf{r}^2}, \quad (32)$$

where the length scale  $\tau$  is given by the lattice spacing. For less symmetric lattice types this expression is not strictly correct but the leading, logarithmic term is always present.<sup>29</sup> We here only keep the logarithmic term. The qualitative behavior and the universal jump in the stiffness are known to be unaffected by this.<sup>28,29</sup>

[However, the temperature dependence of the correlation length above the dislocation unbinding transition changes for the triangular lattice as a result of both the sub-leading term in Eq. (32) and the appearance of triplets of dislocations with vanishing total Burger's vector.<sup>28,29</sup>]

As discussed in the introduction, dislocations attract partial vortices to minimize the energy resulting from the mismatch in the antiferromagnetic order. In a Coulomb gas language we have three charges: the vortex strength and the  $x$  and  $y$  components of the dislocation Burger's vector. These three charges correspond to the three gauge fields discussed in Sec. IB. A similar description can be used for the possible upper melting transition from a liquid crystal to an isotropic fluid. This transition is thought to be due to unbinding pairs of disclinations, which may again bind partial vortices.

The model is defined as follows: There are  $N$  species of particles, counted by  $n = 1, \dots, N$ , which carry  $M$  charges  $q_n^1, \dots, q_n^M$ . Each particle has an antiparticle with all charges inverted,  $q_{\bar{n}}^m = -q_n^m$ , where we use the notation  $\bar{n}$  for the species of the antiparticle. The charges interact via the two-dimensional logarithmic Coulomb potential. The interaction between two particles of species  $n$  and  $n'$  at positions  $\mathbf{r}$  and  $\mathbf{r}'$  is then

$$V = - \sum_{m=1}^M q_n^m q_{n'}^m \ln \frac{|\mathbf{r} - \mathbf{r}'|}{\tau}. \quad (33)$$

The charges have units of a square root of energy—the strength of the interaction is contained in  $q_n^m$ . Furthermore, we assume (i) that only a particle and its antiparticle can form a pair that is neutral with respect to *all* charges and (ii) that the whole system is neutral with respect to all charges. The number of  $n$  particles and  $\bar{n}$  antiparticles is then equal. Restriction (i) is in fact not crucial but simplifies the argumentation.

The usual Coulomb gas model for vortices in the  $XY$  model or a superfluid film is the case  $N = 1$ ,  $M = 1$ . Melting of a square lattice without additional degrees of freedom can be described by an  $N = 2$ ,  $M = 2$  Coulomb gas, which reduces to two independent, identical  $N = 1$ ,  $M = 1$  models since dislocations with Burger's vectors along the  $x$  and  $y$  axes, respectively, do not interact. Tupitsyn *et al.*<sup>48</sup> have considered an  $N = 2$ ,  $M = 2$  model for merons in a double-layer quantum Hall system, but with a  $1/r$  interaction for one of the charges.

For the square skyrmion lattice we have  $M = 3$  charges and  $N = 5$  particle species. The charges correspond to the vortex strength ( $q_n^1$ ), the  $x$  component of the Burger's vector ( $q_n^2$ ), and its  $y$  component ( $q_n^3$ ). The charges of the particles are given in table I. This table reflects the fact that dislocations bind  $+1/2$  or  $-1/2$  vortex.

We apply Kosterlitz' renormalization group formulation<sup>27</sup> of BKT theory to the general  $N$ ,  $M$  model. This approach has the advantage of being more rigorous and mathematically more transparent than, *e.g.*, the original

self-consistent screening approach.<sup>26,46</sup> The renormalization procedure of Ref. 27 consists of two steps: First, the smallest neutral pair is integrated out, and then the length scale  $\tau$ , the size of the smallest pairs, is rescaled. The procedure for the multiple-charge Coulomb gas is similar to the original case<sup>27</sup> and is not given in detail.

The main approximation of the original theory<sup>27</sup> is that the two particles with smallest separation are assumed to *always* form a neutral pair. This is reasonable since two particles which do not form a neutral pair have the same charge and thus repel each other. In our case this is not generally true: two particles which are not a neutral pair can even attract each other and form a non-neutral bound state. However, this arrangement will attract other particles until it is totally neutral. The approximation that the smallest pair is neutral is thus equivalent to neglecting neutral arrangements of more than two particles. The same problem arises for the triangular lattice without  $XY$  degree of freedom, where three elementary dislocations can have vanishing total Burger's vector.<sup>29</sup> Depending on the  $q_n^m$  there can be neutral triplets, *e.g.*,  $(1\bar{2}3)$  in the above example, whereas in the  $N = 1$  case the simplest neutral arrangements except for pairs are quartets. Therefore the first neglected term in the renormalization group equations is of fourth order in the particle fugacities for both the  $XY$  model on a rigid lattice<sup>49</sup> and the melting square lattice without  $XY$  degree of freedom, whereas it is of third order for the square skyrmion lattice.

The grand canonical partition function of the multiple-charge Coulomb gas is

$$Z = \sum_{\mathcal{N}_1, \dots, \mathcal{N}_N} \prod_{n=1}^N \left[ \frac{1}{(\mathcal{N}_n!)^2} \left( \frac{y_n}{\tau^2} \right)^{2\mathcal{N}_n} \right] \int_{D_1(\tau)} d^2 r_1 \dots \int_{D_{2\mathcal{N}}(\tau)} d^2 r_{2\mathcal{N}} \exp \left( + \frac{\beta}{2} \sum_{i \neq j} \sum_{m=1}^M q_{n_i}^m q_{n_j}^m \ln \frac{|\mathbf{r}_i - \mathbf{r}_j|}{\tau} \right), \quad (34)$$

where  $\mathcal{N}_n$  is the number of particles of species  $n$  (there is the same number of  $\bar{n}$  antiparticles),  $\mathcal{N} = \sum_n \mathcal{N}_n$ , the  $y_n$  are fugacities, the ranges of integration  $D_i(\tau)$  comprise the whole plane but exclude configurations with two particles closer than  $\tau$ , and the double sum  $\sum_{i \neq j}$  runs over all  $2\mathcal{N}$  particles and antiparticles. Pairs of size in  $[\tau, \tau + d\tau)$  are integrated out according to

$$\prod_{i=1}^{2\mathcal{N}} \int_{D_i(\tau)} d^2 r_i \cong \prod_{i=1}^{2\mathcal{N}} \int_{D_i(\tau+d\tau)} d^2 r_i + \frac{1}{2} \sum_{i \neq j} \prod_{k \neq i, j} \int_{D_k(\tau+d\tau)} d^2 r_k \int_{D'} d^2 r_j \times \int_{\tau \leq |\mathbf{r}_i - \mathbf{r}_j| < \tau + d\tau} d^2 r_i \delta_{n_i, \bar{n}_j}. \quad (35)$$

Here,  $D'$  consists of the whole plane except for disks of radius  $\tau$  centered at all particles  $k \neq i, j$ . The only ap-

proximation here is contained in the symbol  $\delta_{n_i, \bar{n}_j}$ , which states that only neutral pairs are integrated out. Applying this prescription to Eq. (34) and rescaling  $\tau$  we obtain (cf. Ref. 27)

$$Z \cong Z_0 \sum_{\mathcal{N}_1, \dots, \mathcal{N}_N} \prod_{n=1}^N \left[ \frac{1}{(\mathcal{N}_n!)^2} \left( \frac{y_n}{(\tau + d\tau)^2} \right)^{2\mathcal{N}_n} \times \left( 1 + [2 - \beta/2 \sum_{m=1}^M (q_n^m)^2] \frac{d\tau}{\tau} \right)^{2\mathcal{N}_n} \right] \times \prod_{i=1}^{2\mathcal{N}} \int_{D_i(\tau+d\tau)} d^2 r_i \exp \left( + \frac{\beta}{2} \sum_{i \neq j} \left[ \sum_{m=1}^M q_{n_i}^m q_{n_j}^m - 2\pi^2 \sum_{n=1}^N y_n^2 \frac{d\tau}{\tau} \beta \left( \sum_{m=1}^M q_{n_i}^m q_n^m \right) \left( \sum_{m=1}^M q_n^m q_{n_j}^m \right) \right] \right) \times \ln \frac{|\mathbf{r}_i - \mathbf{r}_j|}{\tau + d\tau}. \quad (36)$$

Except for the irrelevant constant  $Z_0$ , this partition function is identical to the original one if we replace

$$y_n \rightarrow \left[ 1 + \left( 2 - \frac{\beta}{2} \sum_{m=1}^M (q_n^m)^2 \right) \frac{d\tau}{\tau} \right] y_n, \quad (37)$$

$$\sum_{m=1}^M q_n^m q_{n'}^m \rightarrow \sum_{m=1}^M q_n^m q_{n'}^m - 2\pi^2 \sum_{n''=1}^N y_{n''}^2 \beta \times \left( \sum_{m=1}^M q_n^m q_{n''}^m \right) \left( \sum_{m=1}^M q_{n''}^m q_{n'}^m \right) \frac{d\tau}{\tau}. \quad (38)$$

If we define a (symmetric) stiffness tensor

$$K_{nn'} \equiv \frac{\beta \sum_m q_n^m q_{n'}^m}{2\pi} \quad (39)$$

and express the scaling relations for  $y_n$  and  $K_{nn'}$  by differential equations, we obtain the generalized renormalization group equations

$$\frac{dy_n^2}{d\ell} = 2(2 - \pi K_{nn}) y_n^2, \quad (40)$$

$$\frac{dK_{nn'}}{d\ell} = -4\pi^3 \sum_{n''=1}^N y_{n''}^2 K_{nn''} K_{n''n'}, \quad (41)$$

where  $\ell = \ln r/\tau$  is the logarithmic length scale. The initial conditions for these equations are

$$y_n^2(\ell = 0) = C_n^2 e^{-2\beta E_n^{\text{core}}}, \quad (42)$$

$$K_{nn'}(\ell = 0) = \frac{\beta \sum_m q_n^m(0) q_{n'}^m(0)}{2\pi}, \quad (43)$$

where  $C_n$  are constants of the order of unity and  $E_n^{\text{core}}$  are the core energies of one  $n$  particle. Note that the generalized Kosterlitz equations and the initial conditions reduce to the standard BKT expressions for  $N = 1, M = 1$ .

## B. Skyrmion lattices

We first consider the square skyrmion lattice ( $N = 5$ ,  $M = 3$ ). At first glance this problem looks rather complicated, since it involves coupled differential equations in 5 fugacities and 15 stiffness constants, taking the symmetry of  $K_{nn'}$  into account. However, we can simplify the problem considerably by looking for further symmetries. In a first step we consider the symmetries of  $y_n$  and  $K_{nn'}$  at the minimum length scale  $\ell = 0$  and check which of these survive for the renormalized quantities at  $\ell > 0$ . From table I and the observation that the core energies of all species of dislocations should be equal, we see that at  $\ell = 0$  there are at most seven independent quantities,

$$\begin{aligned}
y_v &\equiv y_1, \\
y_d &\equiv y_2 = y_3 = y_4 = y_5, \\
K_v &\equiv K_{11}, \\
K_d &\equiv K_{22} = K_{33} = K_{44} = K_{55}, \\
K_{vd} &\equiv K_{12} = -K_{13} = K_{14} = -K_{15}, \\
K'_{dd} &\equiv K_{23} = K_{45}, \\
K''_{dd} &\equiv K_{24} = -K_{25} = -K_{34} = K_{35}.
\end{aligned} \tag{44}$$

The equations for these quantities can be read off from Eqs. (40) and (41). It is easy to see that two quantities that are equal by symmetry at  $\ell = 0$  remain equal to each other as we integrate away from  $\ell = 0$ . Hence, the problem can be reduced to seven coupled equations,

$$\begin{aligned}
dy_v^2/d\ell &= 2(2 - \pi K_v) y_v^2, \\
dy_d^2/d\ell &= 2(2 - \pi K_d) y_d^2, \\
dK_v/d\ell &= -4\pi^3 y_v^2 K_v^2 - 16\pi^3 y_d^2 K_{vd}^2, \\
dK_d/d\ell &= -4\pi^3 y_v^2 K_{vd}^2 - 4\pi^3 y_d^2 (K_d^2 + K_{dd}^2 + 2K'_{dd}), \\
dK_{vd}/d\ell &= -4\pi^3 y_v^2 K_v K_{vd} \\
&\quad - 4\pi^3 y_d^2 (K_d K_{vd} - K_{dd} K_{vd} + 2K'_{dd} K_{vd}), \\
dK_{dd}/d\ell &= +4\pi^3 y_v^2 K_{vd}^2 - 8\pi^3 y_d^2 (K_d K_{dd} - K'_{dd}), \\
dK'_{dd}/d\ell &= -4\pi^3 y_v^2 K_{vd}^2 - 8\pi^3 y_d^2 (K_d K'_{dd} - K_{dd} K'_{dd}).
\end{aligned} \tag{45}$$

In a second step we make an ansatz for the remaining  $K$  to reduce the number of independent quantities further. We *guess* that the renormalization of the interactions can be described in terms of independent screening of the two charges  $q_v$  and  $q_d$  alone (we will see below that this assumption is not correct for all lattice types). If it were true there would be only two independent stiffness constants  $J_v$  and  $J_d$ , which we choose so that

$$J_v(0) = \frac{\beta q_v^2(0)}{2\pi}, \quad J_d(0) = \frac{\beta q_d^2(0)}{2\pi}. \tag{46}$$

Since our ansatz has to work at  $\ell = 0$  we have

$$\begin{aligned}
K_v &= J_v, \\
K_d &= J_d + J_v/4, \\
K_{vd} &= J_v/2, \\
K_{dd} &= J_d - J_v/4, \\
K'_{dd} &= J_v/4.
\end{aligned} \tag{47}$$

Inserting this ansatz into Eqs. (45) we obtain four independent equations,

$$dy_v^2/d\ell = 2(2 - \pi J_v) y_v^2, \tag{48}$$

$$dy_d^2/d\ell = 2(2 - \pi J_d - \pi J_v/4) y_d^2, \tag{49}$$

$$dJ_v/d\ell = -4\pi^3 y_v^2 J_v^2 - 4\pi^3 y_d^2 J_v^2, \tag{50}$$

$$dJ_d/d\ell = -8\pi^3 y_d^2 J_d^2, \tag{51}$$

and three that are linear combinations of these. Thus our ansatz is indeed correct. Of course, we could have made this ansatz directly for the  $K_{nn'}$  without the step in between. We repeat that the leading neglected terms in Eqs. (48)–(51) are of third order in  $y_{v,d}$ .

From Eqs. (50) and (51) we see immediately that if the dislocations proliferate,  $\lim_{\ell \rightarrow \infty} y_d^2 = \infty$ , both stiffness constants  $J_v$  and  $J_d$  go to zero for  $\ell \rightarrow \infty$ . This result reflects the fact that free dislocations do not only screen the dislocation interaction but also the vortex interaction since they carry vorticity. On the other hand, free vortices ( $\lim_{\ell \rightarrow \infty} y_v^2 = \infty$ ) only lead to  $J_v \rightarrow 0$  since vortices do not have a non-zero Burger's vector, and, consequently, Eq. (51) does not contain  $y_v^2$ . We now discuss the possible scenarios.

*Decoupled transitions*, Fig. 4(a): We start from low temperatures. At some temperature  $T_v$ , vortices unbind and  $J_v(\ell \rightarrow \infty)$  shows a universal jump from  $2/\pi$  to zero. (We now omit the  $\ell$  argument when we refer to the limit  $\ell \rightarrow \infty$ .) At the same temperature the *effective* stiffness of the dislocation interaction,  $J_d + J_v/4$ , also shows a jump but at the high-temperature side  $T_v^+$  of the jump we still have  $J_d + J_v/4 = J_d > 2/\pi$ . There is no jump in  $J_d$  alone. Above  $T_v$  the system has only short-range magnetic order but still quasi-long-range translational order. At some higher temperature  $T_d$  the dislocations unbind and  $J_d$  jumps from  $2/\pi$  to zero. Both transitions show BKT finite size scaling,<sup>46</sup>  $J_{v,d}(\ell, T_{v,d}) \cong 2/\pi[1 + 1/(2\ell)]$ .

*Vortex driven simultaneous transitions*, Fig. 4(b): At  $T_v$  vortices unbind:  $J_v$  jumps from  $2/\pi$  to zero. At  $T_v^-$ , the effective dislocation stiffness is  $J_d + J_v/4 > 2/\pi$ , while  $J_d$  alone is smaller than  $2/\pi$ . With  $J_v$  jumping to zero, we appear to have  $J_d + J_v/4 = J_d < 2/\pi$  at  $T_v^+$ , see the cross in Fig. 4(b). However, from Eq. (49) we see that then  $\lim_{\ell \rightarrow \infty} y_d = \infty$ , dislocations also proliferate, and  $J_d$  jumps to zero. The physical reason is that with the vortex interaction screened the remaining dislocation interaction is suddenly too weak to bind dislocation pairs so that  $T_d = T_v$ . We expect BKT scaling only in  $J_v$ .

*Dislocation driven simultaneous transitions*, Fig. 4(c): At  $T_d$  dislocations unbind: the effective stiffness  $J_d + J_v/4$  jumps from  $2/\pi$  to zero. The vortex stiffness is still large at  $T_d^-$ ,  $J_v(T_d^-) > 2/\pi$  so that vortices would unbind at a higher temperature. However, since  $J_d + J_v/4$  vanishes at  $T_d^+$ , so does  $J_v$  so that  $T_v = T_d$ . Physically, the vortex interaction is suddenly screened since the proliferating dislocations carry vorticity. For this reason the magnetic transition can never take place at a higher temperature than the melting. There can be lattice order without magnetic order but not *vice versa*. We expect

BKT scaling in  $J_d + J_v/4$  and also find similar scaling in  $J_v$  and  $J_d$  separately but with a non-universal value of  $J_{v,d}(T_d^-) \neq 2/\pi$ .

Above the dislocation unbinding transition at  $T_d$  the system still shows orientational quasi-long-range order, whereas translational and magnetic order are of short range. This is the tetratic phase mentioned in the introduction.<sup>28</sup> It is characterized by free dislocations, which are in fact bound pairs of disclinations.<sup>28</sup> For the square lattice elementary *bare* disclinations do not carry vorticity, as can be seen from Fig. 5. Disclinations dress with free dislocations, leading to a logarithmic interaction.<sup>28</sup> This screening cloud of dislocations is expected to have vanishing total Burger's vector and vanishing total vorticity in order to minimize its energy. Thus dressed disclinations still have zero Burger's vector and vortex strength and the disclination unbinding transition corresponds to an  $N = 1, M = 1$  model with the dressed fivefold disclination as the particle and the dressed threefold disclination as its antiparticle. At a temperature  $T_{\text{disc}} > T_d$  disclination pairs unbind and the system becomes an isotropic fluid.

We now turn to the other lattice types. The triangular lattice has dislocations with Burger's vectors along any of three axes. Dislocations lead to a phase mismatch of  $\pm 2\pi/3$  in the frustrated ( $120^\circ$ ) magnetic order and thus attract  $\pm 1/3$  vortex. Consequently, there are six species of dislocations: three directions of Burger's vectors and two signs of the vorticity. Dislocations with Burger's vectors in different directions now interact, the interaction is proportional to the cosine of the angle between them,<sup>28</sup> cf. Eq. (32). The charges are given in table II. All species of dislocations are equivalent and the final equations are

$$dy_v^2/dl = 2(2 - \pi J_v) y_v^2, \quad (52)$$

$$dy_d^2/dl = 2(2 - \pi J_d - \pi J_v/9) y_d^2, \quad (53)$$

$$dJ_v/dl = -4\pi^3 y_v^2 J_v^2 - (8/3)\pi^3 y_d^2 J_v^2, \quad (54)$$

$$dJ_d/dl = -12\pi^3 y_d^2 J_d^2. \quad (55)$$

Note that there are no neutral triplets in the triangular skyrmion lattice, as opposed to the usual triangular lattice. Thus the first omitted terms are of fourth order in the fugacities.<sup>50</sup> Eqs. (52)–(55) differ from the square lattice case only in the coefficients. The possible melting regimes are thus qualitatively the same. The liquid crystal phase is hexatic.<sup>28</sup> Bare disclinations do carry vorticity ( $\pm 1/3$ ) but this fact is irrelevant for the upper transition since the vorticity part of the disclination interaction is totally screened by free vortices and dislocations.

The centered rectangular lattice can be generated from the square lattice by tilting the angle  $\theta$  between the primitive lattice vectors away from  $\theta = \pi/2$  but keeping their lengths fixed. This tilting leads to an interaction between dislocations with Burger's vectors along different primitive vectors. However, all elementary dislocations still have the same fugacity and effective interaction with their respective antiparticles since they are related by reflection symmetry. The charges are given in table III.

For  $\theta = \pi/2$  we recover the square lattice. Our usual ansatz, which assumes that the system can be described in terms of screening of  $q_v$  and  $q_d$  alone, fails here. We cannot reduce the problem to four coupled equations for general values of  $\phi$  but need five:

$$dy_v^2/dl = 2(2 - \pi J_v) y_v^2, \quad (56)$$

$$dy_d^2/dl = 2(2 - \pi J_+/2 - \pi J_-/2 - \pi J_v/4) y_d^2, \quad (57)$$

$$dJ_v/dl = -4\pi^3 y_v^2 J_v^2 - 4\pi^3 y_d^2 J_v^2, \quad (58)$$

$$dJ_\pm/dl = -8\pi^3 y_d^2 J_\pm^2 \quad (59)$$

with the initial conditions for the  $J$

$$J_v(0) = \beta q_v^2(0)/2\pi, \quad (60)$$

$$J_\pm(0) = (1 \pm \cos \phi) \beta q_d^2(0)/2\pi. \quad (61)$$

Nevertheless there can be at most two transitions (apart from disclination unbinding) since there are only two fugacities. The possible regimes are the same as for the square lattice if we replace  $J_d$  by  $(J_+ + J_-)/2$ . Above the lower melting transition the system is in a liquid crystal phase with quasi-long-range orientational order with respect to a *twofold* symmetry. This is a two-dimensional *nematic* phase. Elementary disclinations do not carry vorticity so that the upper melting transition is simple.

The simple rectangular lattice is generated from the square lattice by stretching it in the (10) direction. Dislocations with Burger's vectors in the  $x$  and  $y$  direction, respectively, now have different energies, increasing the number of independent variables. Dislocations still bind  $\pm 1/2$  vortex. There are again  $N = 5$  particles and  $M = 3$  charges. The final renormalization group equations are

$$dy_v^2/dl = 2(2 - \pi J_v) y_v^2, \quad (62)$$

$$dy_{d1}^2/dl = 2(2 - \pi J_{d1} - \pi J_v/4) y_{d1}^2, \quad (63)$$

$$dy_{d2}^2/dl = 2(2 - \pi J_{d2} - \pi J_v/4) y_{d2}^2, \quad (64)$$

$$dJ_v/dl = -4\pi^3 y_v^2 J_v^2 - 2\pi^3 y_{d1}^2 J_v^2 - 2\pi^3 y_{d2}^2 J_v^2, \quad (65)$$

$$dJ_{d1}/dl = -8\pi^3 y_{d1}^2 J_{d1}^2, \quad (66)$$

$$dJ_{d2}/dl = -8\pi^3 y_{d2}^2 J_{d2}^2. \quad (67)$$

Since the dislocation energies are different, there are two distinct dislocation unbinding transitions at  $T_{d1}$  and  $T_{d2}$  except if they are driven by vortex unbinding. If there are two structural transitions, the phase between them has translational quasi-long-range order in, say, the  $x$  direction, but short-range order in the  $y$  direction. It is thus a two-dimensional *smectic* phase. There are five possible scenarios, which follow from our considerations for the square lattice and are not discussed here. For  $T > \max(T_{d1}, T_{d2})$  we again have a nematic phase (twofold rotational symmetry). Elementary disclinations do not carry vorticity and the upper melting transition is simple.

The lower melting transition of the honeycomb lattice is trivial in this context since its dislocations do not carry vorticity: The structural lattice has the same basis as the magnetic lattice so that dislocations (with any Burger's vector) cannot lead to a phase mismatch. Thus

antiferromagnetic quasi-long-range order could persist in the liquid crystal phase above the dislocation unbinding transition, which is expected to have unique properties.<sup>43</sup> Disclinations carry  $\pm 1/2$  vortex and any remaining magnetic order is destroyed at the upper melting transition.

Finally we stress again that these considerations can only yield the possible sequence of *BKT transitions* for any lattice type. This approach cannot describe other transitions directly, such as first-order melting transitions<sup>28</sup> or first or second-order structural transitions. Structural transitions in particular could take place since magnetic disordering leads to a reduced effective magnetic interaction between skyrmions, affecting the stability of the various lattice types in different ways.

In fact, the question arises of whether the square skyrmion lattice can be stable at all above the magnetic disordering transition. The answer is affirmative since the magnetic part of the interaction is of short range: As long as the magnetic BKT correlation length  $\xi_v$ , which for  $T \gtrsim T_c$  satisfies<sup>26,46</sup>

$$\frac{\xi_v(T)}{\tau} \cong \exp\left(\frac{b}{\sqrt{T - T_c}}\right), \quad (68)$$

is much larger than the range of the magnetic interaction,  $\xi_{XY}$ , the effect of magnetic disordering on the lattice energies is negligible. Only when, at a higher temperature,  $\xi_v$  becomes comparable to  $\xi_{XY}$ , frustration becomes important. In this case we expect the magnetic interaction to be effectively reduced so that eventually the triangular lattice becomes favorable. If at  $T = T_d$  still  $\xi_v \gtrsim \xi_{XY}$ , the square lattice melts and forms a tetratic phase before a structural transition takes place. It can even exhibit the upper melting transition without any structural transition taking place, depending on the non-universal constant  $b$  in Eq. (68). The same kind of argument holds for other lattice and liquid crystal structures.

#### IV. CONCLUSIONS

As noted above, the lattice types relevant for present quantum Hall systems are the triangular, centered rectangular, and square lattices. A rough estimate of the actual core energies and interactions in the real quantum Hall system using the model of Sec. II A and results of Ref. 35 indicates that the low-density, triangular lattice typically shows decoupled magnetic and melting transitions, cf. Fig. 4(a). The magnetic skyrmion interaction, and thus the magnetic stiffness and the vortex energies, are small since a strong magnetic interaction would make the triangular lattice unstable. The effective magnetic stiffness is further reduced by frustration.

On the other hand, the centered rectangular and square lattices usually show simultaneous transitions, *i.e.*, magnetic order persists up to the lower melting temperature. Experimentally, the two possible scenarios of Figs. 4(b) and (c) are probably not easy to distinguish.

Note also that vortex driven simultaneous transitions, Fig. 4(b), require fine tuning of magnetic and structural stiffnesses so that this scenario is probably rare.

Quantum fluctuations can affect these results. As noted above they are expected to lead to quantum melting in the vicinity of the classical square-centered rectangular line. They should also destroy magnetic order in the triangular lattice at sufficiently low densities, where the magnetic interaction becomes exponentially small. More experiments are needed to test the predictions of this paper. Sharp structures in the Knight shift, nuclear relaxation rates, or specific heat as functions of temperature would be indications for phase transitions of the skyrmion system. Particularly valuable would be experiments on the electronic susceptibility  $\chi(\mathbf{q}, \omega)$  as a function of temperature and filling factor.

In conclusion, we have performed a Berezinskii-Kosterlitz-Thouless renormalization group study of melting and magnetic disordering in various lattice geometries in order to understand the behavior of the skyrmion lattice in quantum Hall ferromagnets at finite temperatures. The behavior of the skyrmion system is determined by the two facts that skyrmions (i) are non-collinear magnetic defects and (ii) carry electrical charge. In the long-wavelength limit the in-plane magnetization components can be described by a U(1) (*XY*) degree of freedom associated with each skyrmion. The *XY* “spins” couple antiferromagnetically and can lead to antiferromagnetic quasi-long-range order. Dislocations in most skyrmion lattice types lead to a mismatch in the *XY* degree of freedom, which makes the dislocations bind fractional vortices and leads to coupling of translational and magnetic excitations. For most lattice types there are three distinct scenarios for the lower melting transition: (i) a BKT magnetic disordering transition at a lower temperature than BKT melting, (ii) simultaneous transitions where the magnetic stiffness shows a universal BKT jump, and (iii) simultaneous transitions where the effective dislocation stiffness shows a universal jump.

The lattice types we have studied are motivated by the possible ground states of a simple classical model of the skyrmion system, which uses the large-separation limit of their interaction. It shows a surprisingly rich  $T = 0$  phase diagram, which suggests that upon increasing the skyrmion density a frustrated triangular ground state first gives way to a centered rectangular lattice with Néel order and only at higher density to a square lattice. Quantum melting is expected to take place in the vicinity of the latter transition.

#### ACKNOWLEDGMENTS

We wish to thank A.H. MacDonald, S.E. Barrett, and S. Sachdev for valuable discussions. This work has been supported by NSF DMR-9714055, NSF CDA-9601632, and NSF DMR-9503814. C.T. acknowledges support by

the Deutsche Forschungsgemeinschaft. H.A.F. acknowledges a Cottrell Scholar Award of Research Corporation.

---

\* Present address: Freie Universität Berlin, Fachbereich Physik, Arnimallee 14, D-14195 Berlin, Germany.

<sup>1</sup> *The Quantum Hall Effect*, 2nd edition, edited by R.E. Prange and S.M. Girvin (Springer, New York, 1990).

<sup>2</sup> *Quantum Hall Effect: A Perspective*, edited by A.H. MacDonald (Kluwer, Boston, 1989).

<sup>3</sup> T. Chakraborty and P. Pietiläinen, *The Quantum Hall Effects* (Springer, New York, 1995).

<sup>4</sup> *The Quantum Hall Effect*, edited by M. Stone (World Scientific, Singapore, 1992).

<sup>5</sup> *Perspectives in Quantum Hall Effects: Novel Quantum Liquids in Low-Dimensional Semiconductor Structures*, edited by S. Das Sarma and A. Pinczuk (Wiley, New York, 1997).

<sup>6</sup> B.I. Halperin, *Helv. Phys. Acta* **56**, 75 (1983).

<sup>7</sup> A.H. MacDonald, *Surface Science* **229**, 1 (1990).

<sup>8</sup> X.G. Wen and A. Zee, *Phys. Rev. Lett.* **69**, 1811 (1992).

<sup>9</sup> K. Yang, K. Moon, L. Zheng, A.H. MacDonald, S.M. Girvin, D. Yoshioka, and S.-C. Zhang, *Phys. Rev. Lett.* **72**, 732 (1994).

<sup>10</sup> K. Moon, H. Mori, K. Yang, S.M. Girvin, A.H. MacDonald, L. Zheng, D. Yoshioka, and S.-C. Zhang, *Phys. Rev. B* **51**, 5138 (1995).

<sup>11</sup> V. Pellegrini, A. Pinczuk, B.S. Dennis, A.S. Plaut, L.N. Pfeiffer, and K.W. West, *Phys. Rev. Lett.* **78**, 310 (1997).

<sup>12</sup> S. Das Sarma, S. Sachdev, and L. Zheng, *Phys. Rev. Lett.* **79**, 917 (1997).

<sup>13</sup> S.M. Girvin and A.H. MacDonald, in Ref. 5.

<sup>14</sup> S.E. Barrett, G. Dabbagh, L.N. Pfeiffer, K.W. West, and R. Tycko, *Phys. Rev. Lett.* **74**, 5112 (1995); R. Tycko, S.E. Barrett, G. Dabbagh, L.N. Pfeiffer, K.W. West, *Science* **268**, 1460 (1995).

<sup>15</sup> V. Bayot, E. Grivei, S. Melinte, M.B. Santos, and M. Shayegan, *Phys. Rev. Lett.* **76**, 4584 (1996).

<sup>16</sup> S.L. Sondhi, A. Karlhede, S.A. Kivelson, and E.H. Rezayi, *Phys. Rev. B* **47**, 16419 (1993).

<sup>17</sup> R. Côté, A.H. MacDonald, L. Brey, H.A. Fertig, S.M. Girvin, and H.T.C. Stoof, *Phys. Rev. Lett.* **78**, 4825 (1997).

<sup>18</sup> D.-H. Lee and C.L. Kane, *Phys. Rev. Lett.* **64**, 1313 (1990).

<sup>19</sup> T.H.R. Skyrme, *Proc. Royal Soc.* **A262**, 233 (1961).

<sup>20</sup> A.A. Belavin and A.M. Polyakov, *Pis'ma Zh. Eksp. Teor. Fiz.* **22**, 503 (1975) [*JETP Lett.* **22**, 245 (1975)].

<sup>21</sup> R. Rajaraman, *Solitons and Instantons* (North-Holland, Amsterdam, 1989).

<sup>22</sup> H.A. Fertig, L. Brey, R. Côté, and A.H. MacDonald, *Phys. Rev. B* **50**, 11018 (1994); A.H. MacDonald, H.A. Fertig, and L. Brey, *Phys. Rev. Lett.* **76**, 2153 (1996); H.A. Fertig, L. Brey, R. Côté, A.H. MacDonald, A. Karlhede, and S.L. Sondhi, *Phys. Rev. B* **55**, 10671 (1997).

<sup>23</sup> L. Brey, H.A. Fertig, R. Côté, and A.H. MacDonald, *Phys. Rev. Lett.* **75**, 2562 (1995).

<sup>24</sup> M. Rao, S. Sengupta, and R. Shankar, *Phys. Rev. Lett.* **79**, 3998 (1997).

<sup>25</sup> A.G. Green, I.I. Kogan, and A.M. Tsvetlik, *Phys. Rev. B* **54**, 16838 (1996).

<sup>26</sup> V.L. Berezinskii, *Zh. Eksp. Teor. Fiz.* **61**, 1144 (1971) [*Sov. Phys. JETP* **34**, 610 (1972)]; J.M. Kosterlitz and D.J. Thouless, *J. Phys. C* **6**, 1181 (1973).

<sup>27</sup> J.M. Kosterlitz, *J. Phys. C* **7**, 1046 (1974).

<sup>28</sup> D.R. Nelson, *Phys. Rev. B* **18**, 2318 (1978); D.R. Nelson and B.I. Halperin, *Phys. Rev. B* **19**, 2457 (1979).

<sup>29</sup> A.P. Young, *Phys. Rev. B* **19**, 1855 (1979).

<sup>30</sup> The Lorentz force mixes the transverse acoustical phonon mode, which has  $\omega_T \propto k$ , with the longitudinal plasmon mode with  $\omega_L \propto k^{1/2}$ . Hence the frequency of the resulting magnetophonon mode is  $\omega = \omega_T \omega_L / \omega_c \propto k^{3/2}$ , where  $\omega_c$  is the cyclotron frequency.

<sup>31</sup> H.T.C. Stoof (unpublished).

<sup>32</sup> J.L. Cardy, M.P.M. den Nijs, and M. Schick, *Phys. Rev. B* **27**, 4251 (1983).

<sup>33</sup> L.D. Landau and E.M. Lifshitz, *Theory of Elasticity*, 3rd english edition (Pergamon, Oxford, 1986).

<sup>34</sup> D.J. Thouless, *J. Phys. C* **11**, L189 (1978).

<sup>35</sup> D.S. Fisher, B.I. Halperin, and R. Morf, *Phys. Rev. B* **20**, 4692 (1979).

<sup>36</sup> A.M. Polyakov, *Phys. Lett.* **59B**, 79 (1975); F.D.M. Haldane, *Phys. Rev. Lett.* **61**, 1029 (1988); J.P. Rodriguez, *Phys. Rev. B* **39**, 2906 (1989); A. Auerbach, B.E. Larson, and G.N. Murthy, *Phys. Rev. B* **43**, 11515 (1991).

<sup>37</sup> A. Auerbach, *Interacting Electrons and Quantum Magnetism* (Springer, New York, 1995).

<sup>38</sup> M. Abolfath, J.J. Palacios, H.A. Fertig, S.M. Girvin, and A.H. MacDonald, *Phys. Rev. B* **56**, 6795 (1997).

<sup>39</sup> P.P. Ewald, *Ann. Phys. (Leipzig)* **54**, 519 (1917); *ibid.* **54**, 557 (1917); *ibid.* **64**, 253 (1921).

<sup>40</sup> L. Bonsall and A.A. Maradudin, *Phys. Rev. B* **15**, 1959 (1977).

<sup>41</sup> G. Goldoni and F.M. Peeters, *Phys. Rev. B* **53**, 4591 (1996).

<sup>42</sup> I.S. Gradshteyn and I.M. Ryzhik, *Table of Integrals, Series, and Products*, 5th edition (Academic, San Diego, 1994).

<sup>43</sup> C. Timm (unpublished).

<sup>44</sup> M. Stone, *Phys. Rev. B* **53**, 16573 (1996).

<sup>45</sup> The classical dynamics calculations are in a sense dual to Ref. 17: Our model is valid in the limit of small skyrmion density, whereas the time-dependent Hartree-Fock calculations work best at high density.

<sup>46</sup> B.I. Halperin, in *Proceedings of Kyoto Summer Institute 1979—Physics of Low-Dimensional Systems*, edited by Y. Nagaoka and S. Hikami (Publication Office, Prog. Theor. Phys., Kyoto, 1979), p. 53.

<sup>47</sup> F.R.N. Nabarro, *Theory of Dislocations* (Clarendon, New York, 1967).

<sup>48</sup> I. Tupitsyn, M. Wallin, and A. Rosengren, *Phys. Rev. B* **53**, R7614 (1996).

<sup>49</sup> The  $y^4$  terms are considered in: D.J. Amit, Y.Y. Goldschmidt, and G. Grinstein, *J. Phys. A* **13**, 585 (1980); C. Timm, *Physica C* **265**, 31 (1996).

<sup>50</sup> Thus the temperature dependence of the correlation length should not be changed by the mechanism discussed by Young, Ref. 29.

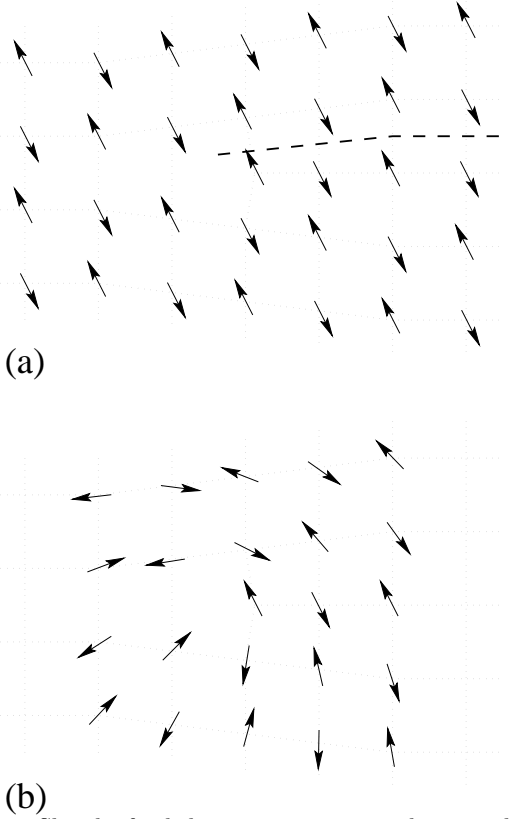


FIG. 1. Sketch of a dislocation in a square skyrmion lattice. The arrows denote the internal U(1) degree of freedom. As seen in (a), dislocations lead to a phase mismatch of  $\pm\pi$  in the U(1) degree of freedom. In (b) the U(1) angles have been allowed to relax and the dislocation has acquired half a vortex.

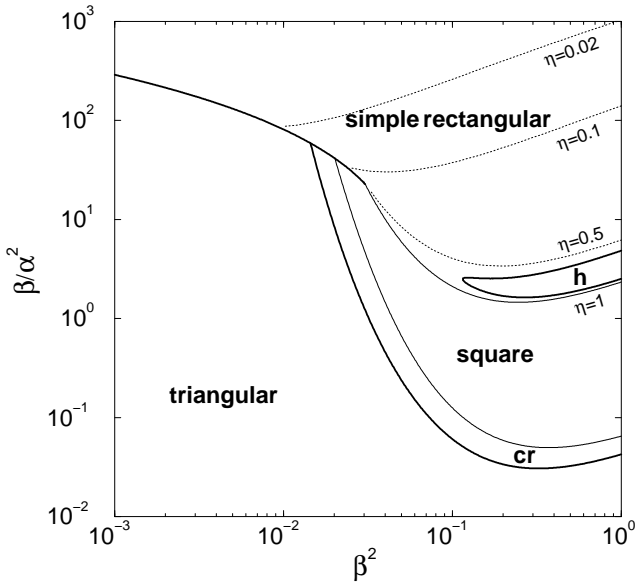


FIG. 2. Classical skyrmion lattice phase diagram at  $T = 0$ . Thin solid lines are continuous phase transitions, whereas heavy lines are first-order transitions. The honeycomb phase is denoted by 'h' and the centered rectangular phase by 'cr.' The dotted lines in the simple rectangular phase are lines of constant anisotropy  $\eta \leq 1$ . The employed model is quantitatively correct for  $\beta^2 \ll 1$ . Also, real systems are expected to have  $\beta/\alpha^2 \lesssim 1$ .

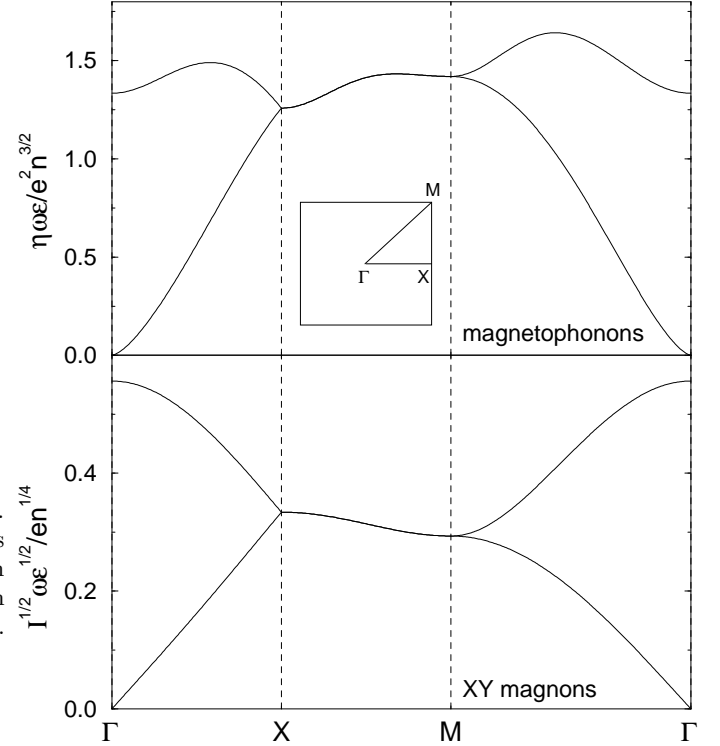


FIG. 3. Dispersion of magnetophonons and XY magnons along high-symmetry directions in the magnetic Brillouin zone of the square skyrmion lattice. The calculation was done for  $\beta^2 = 0.1$  and  $\beta/\alpha^2 = 1$ .

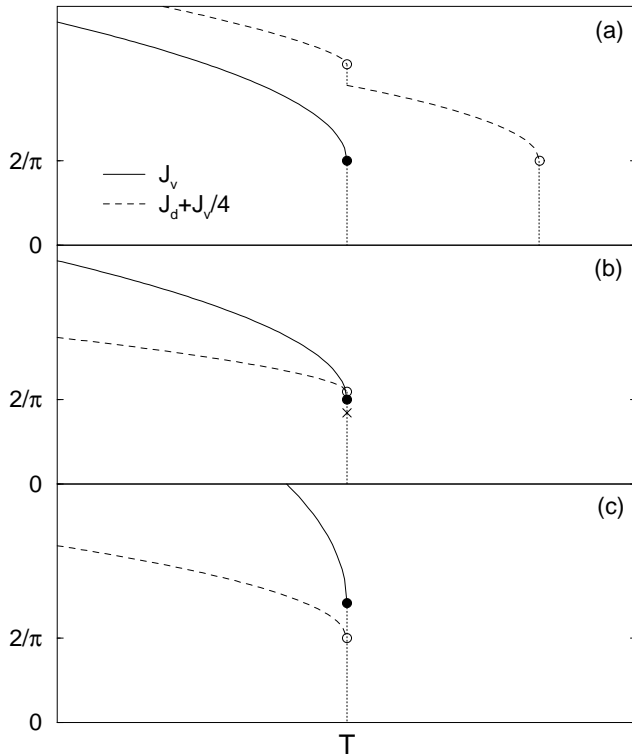


FIG. 4. The three possible scenarios close to the lower melting transition of the square skyrmion lattice: (a) decoupled transitions, (b) vortex driven simultaneous transitions, and (c) dislocation driven simultaneous transitions, see text. The vortex stiffness  $J_v$  and the effective dislocation stiffness  $J_d + J_v/4$  are plotted as functions of temperature. The graphs have not been obtained by actual integration but are rather sketches meant to emphasize the universal features.

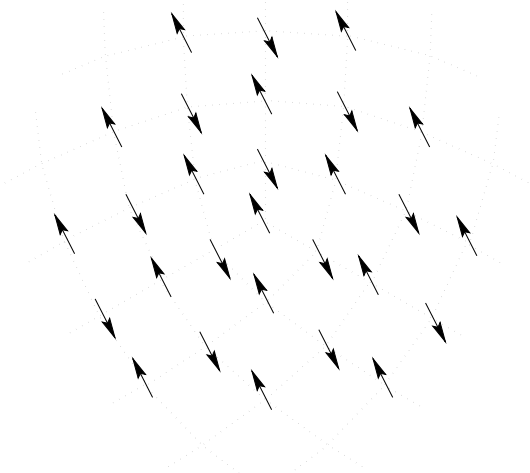


FIG. 5. Sketch of a threefold disclination in the square skyrmion lattice. The disclination does not frustrate the antiferromagnetic order of the  $XY$  spins (arrows).

$n$	$q_n^1$	$q_n^2$	$q_n^3$
1	$q_v$	0	0
2	$q_v/2$	$q_d$	0
3	$-q_v/2$	$q_d$	0
4	$q_v/2$	0	$q_d$
5	$-q_v/2$	0	$q_d$

TABLE I. Coulomb gas charges of the square skyrmion lattice.  $q_v$  is the vortex charge and  $q_d$  is the dislocation charge.

$n$	$q_n^1$	$q_n^2$	$q_n^3$
1	$q_v$	0	0
2	$q_v/3$	$q_d$	0
3	$-q_v/3$	$q_d$	0
4	$q_v/3$	$\cos(2\pi/3)q_d$	$\sin(2\pi/3)q_d$
5	$-q_v/3$	$\cos(2\pi/3)q_d$	$\sin(2\pi/3)q_d$
6	$q_v/3$	$\cos(2\pi/3)q_d$	$-\sin(2\pi/3)q_d$
7	$-q_v/3$	$\cos(2\pi/3)q_d$	$-\sin(2\pi/3)q_d$

TABLE II. Charges for the triangular lattice.

$n$	$q_n^1$	$q_n^2$	$q_n^3$
1	$q_v$	0	0
2	$q_v/2$	$q_d$	0
3	$-q_v/2$	$q_d$	0
4	$q_v/2$	$\cos(\theta)q_d$	$\sin(\theta)q_d$
5	$-q_v/2$	$\cos(\theta)q_d$	$\sin(\theta)q_d$

TABLE III. Charges for the centered rectangular lattice.